How strongly are the magnetic anisotropy and coordination numbers correlated in lanthanide based molecular magnets?

TULIKA GUPTA and GOPALAN RAJARAMAN*

Department of Chemistry, Indian Institute of Technology Bombay, Powai, Mumbai 400 076, India
e-mail: rajaraman@chem.iitb.ac.in

Abstract. *Ab initio* CASSCF+RASSI-SO investigations on a series of lanthanide complexes [Ln^{III} = Dy(**1**), Tb(**2**), Ce(**3**), Nd(**4**), Pr(**5**) and Sm(**6**)] have been undertaken and in selected cases (for **1**, **2**, **3** and **4**) coordination number (C.N.) around the Ln^{III} ion has been gradually varied to ascertain the effect of C.N. on the magnetic anisotropy. Our calculations reveal that complex **3** possesses the highest barrier height for reorientation of magnetisation (U_{eff}) and predict that **3** is likely to exhibit Single Molecule Magnet (SMM) behaviour. Complex **5** on the other hand is predicted to preclude any SMM behaviour as there is no intrinsic barrier for reorientation of magnetization. Ground state anisotropy of all the complexes show mixed behaviour ranging from pure Ising type to fully rhombic behaviour. Coordination number around the lanthanide ion is found to alter the magnetic behaviour of all the lanthanide complexes studied and this is contrary to the general belief that the lanthanide ions are inert and exert small ligand field interaction. High symmetric low-coordinate Ln^{III} complexes are found to yield large U_{eff} values and thus should be the natural targets for achieving very large blocking temperatures.

Keywords. Lanthanides; magnetic anisotropy; coordination number; effective energy barrier, single molecule magnet.

1. Introduction

Since past two decades, Single Molecule Magnets (SMMs) have received appreciable attention owing to their potential applications for the use of high-density magnetic memories, magnetic refrigeration, molecular spintronics and quantum computing devices.[1–6] These potential applications are due to their slow relaxation of magnetization and enhanced effective barrier heights (U_{eff}) for reorientation of magnetization (to date the highest U_{eff} reported is 652 cm^{-1}).[7] These behaviours can be observed when the molecule has large ground spin state with a uniaxial magnetic anisotropy, namely negative zero-field splitting (ZFS) parameter.[6,7] Besides a large ground state, to increase the SMMs energy barrier and blocking temperatures, it is important to perceive a way to control the magnetic anisotropy.[8] Of particular interest in recent years in research area of SMMs[9] is exploration of systems containing only one spin carrier within a molecule and if such molecules exhibit magnetization blockade, these are called as Single Ion Magnets (SIMs).[10–13] Large unquenched orbital angular momentum, significant intrinsic spin-orbit coupling and presence of large number of unpaired electrons make the lanthanides suitable candidates for

attaining large spin-reversal barriers. Besides this, area lanthanide(III) complexes also have important applications in diagnostic and therapeutic radiopharmaceuticals[14] and as luminescent probe to investigate biomedical systems.[15]

In SIMs, magnetic properties are directly connected with the crystal field created by the surrounding ligands. This emphasizes the importance of crystal field environment in the design of novel SIMs.[16–19] In SIMs coordination environment, number, local point group symmetry and ligand field strength together need to be manipulated to obtain large energy barrier. Magnetic anisotropy in these SIMs arise due to interaction between single metal ion and the ligand field, resulting in preferential orientation of the magnetic moment.[20] This eventually generates a strong influence of coordination geometries on SIM properties. Thus, magnetic properties are affected not only by structural and electronic features of the molecule, but also by their surroundings resulting in the spin dynamics method in SIMs to be complex and poorly understood problem.[21] Indeed, these processes can have significant influence on the field dependence of the relaxation time[22] as well as field-induced multiple relaxation processes.[24] Moreover, Lanthanide containing SIMs are attractive for testing synthetic design principles for slow paramagnetic relaxation because their properties can be tuned at will. In general, in a given

crystal field, the ground magnetic state of the complex (characterized by the total angular momentum *J*), splits into ±M_J sub-levels. In some instances, this leads to a J-splitting in which the levels with higher M_J values are stabilized with respect to the levels with lower M_J values. This leads to the appearance of a barrier between the M_J levels explaining superparamagnetic blocking in the SIMs.

Despite enormous synthetic effort expended in making novel examples of lanthanide-based SIMs, clear understanding of the origin of the slow relaxation of the magnetisation and the mechanisms of the Quantum Tunnelling of the Magnetisation (QTM) still remains scarce. Understanding the factors determining the formation of efficient barriers of blocking of magnetization in SIMs is of primary importance for the fast advance of this new research area.[9,25,26] Slow relaxation of magnetization in SIMs can be achieved by effective involvement of anisotropy at the metal sites. Extensive studies[27] on these SIMs based on lanthanides prove their importance due to their large spin-orbit coupling compared to the crystal-field splitting of the magnetic 4f-shell.[28] All these studies have concluded the crucial participation of excited states of the lanthanide ions in the relaxation process of both mononuclear and polynuclear complexes.[16,19,29–34]

The anisotropy axis on the metal ions can be easily determined if the metal centres possess some symmetry elements. Using the angular overlap model,[35] zero-field splitting and the direction of anisotropy axis can be estimated. However such qualitative ligand-field theories are extremely complex[36] for lanthanides complexes rendering less accurate predictions. Although numerous experimental tools such as Inelastic Neutron scattering (INS),[37,38] multifrequency high-field EPR,[39,40] field and orientation dependent magnetic susceptibility have been used to investigate the magnetic anisotropy, none of them suffice to resolve the directions of local anisotropy axes accurately.

The only straightforward way to attain quantitative information about magnetic networks is via fragment quantum chemistry calculations taking spin-orbit coupling into account non-perturbatively. Particularly, the direction of the local anisotropy axis on a metal site is easily gained as the main magnetic axis of the g tensors of the corresponding Kramers doublet. The single-ion properties of the 4f metal ions are difficult to depict due to the shielded nature of the 4f orbitals, resulting in weak exchange interactions. Recent advances in post Hartree-Fock multi-configurational *ab initio* methodology have made accurate quantum chemical calculations on paramagnetic 4f compounds possible.[41] The Complete Active Space Self Consistent Field (CASSCF) method can accurately predict the magnetic properties of lanthanide complexes,[42,43] and calculations of this type have become an indispensable tool for the explanation of increasingly interesting magnetic phenomena.[44] Although CASSCF *ab initio* calculations are extremely versatile and implicitly include all the effects required to elucidate the magnetic properties, the results offer little in the way of chemically intuitive explanations and attainment of reliable results often requires considerable intervention by expert theorists equipped with access to powerful computational resources.

Although higher coordination number around the lanthanide ions are preferred, low coordination number lanthanide complexes had been reported as early as in 1990's,[65] despite no such detailed magnetic study on these complexes. Recently, Tang and co-workers have reported low-valent complexes showing slow magnetisation of relaxation.[66] In the field of lanthanide based SIMs, recently researchers have focussed on two directions: how to enhance the effective barrier height for reorientation of magnetization and to explain the mechanism of versatile thermal relaxation taking place during the reorientation. As crystal field parameter, coordination number and ligation around the Ln^III ion play crucial role in determining the direction of anisotropy, we have decided to play with these parameters with the hope of understanding the aforementioned key points employing computational tools. Considering the recent research trend on lanthanide based SIMs we intend to offer explicit understanding of anisotropy and magnetic relaxation in varied coordination and metallic environment. Hence, here we have performed detailed *ab initio* calculations on monometallic Ln^III [Ln^III = Dy(**1**), Tb(**2**), Ce(**3**), Nd(**4**), Pr(**5**) and Sm(**6**)] crystal structures surrounded by nitrate ligands. Among these, ions with odd number of electrons and half integral angular momentum values (J) are known as Kramers ions (Dy^III, Ce^III, Nd^III and Sm^III) whereas ions with even number of electrons and integral angular momentum values (J) are known as non-Kramers ions (Tb^III and Pr^III). We have calculated effective barrier height, direction of anisotropy for this series. In selected cases, (for **1**, **2**, **3** and **4**) we have gradually varied the coordination number (C.N.) around Ln^III ions from C.N. 12 to C.N. 2 with an aim to observe the effect of coordination number on the magnetic properties of these lanthanide complexes. To keep the same coordination environment across all models structures, all the complexes are modelled with nitrate ions, however synthesis of such complexes would require monodentate ligands such as hydroxide or other ligands.

2. Computational Methodology

MOLCAS 7.8[68] program package has been used to perform post-Hartree-Fock *ab initio* calculations. Using multiconfigurational approach, relativistic effects were treated in two steps, based on Douglas-Kroll Hamiltonian. For the generation of basis sets, scalar terms were included which has been used to determine spin-free wave functions and also energies through the use of the complete active space self-consistent field (CASSCF) method. So, spin-orbit free states were obtained by employing the RASSCF method whereas spin-orbit coupling has been taken into account using RASSI-SO method[69] which uses CASSCF wave functions as the basis sets and multiconfigurational wave functions as input states. The resultant wave functions and energies of the molecular multiplets were used for the calculation of the anisotropic magnetic properties and g tensors of the lowest state using a specially designed routine SINGLE-ANISO.[70] As a consequence, the magnetic properties of a single magnetic ion are calculated by *ab initio* approach in which the spin-orbit coupling is considered non-perturbatively. We have employed [ANO-RCC...7s6p4d2f.] basis set for Ln^{III} {Ln^{III} = Dy, Tb, Ce, Nd, Pr and Sm}, [ANO-RCC... 3s2p.] basis set for N and [ANO-RCC... 2s.] basis set for H throughout our calculations. These ANO-RCC-VDZ basis sets used for all the atoms are taken from ANO-RCC basis library included in MOLCAS 7.8 program package. The active space for $[Dy^{III}(NO_3)_6]^{3-}$ (**1**), is 9 in 7 for the f^9 configuration of Dy^{III} ion. Here we have employed the CASSCF calculations coupled with RASSI-SO procedure to estimate the ground state anisotropy and other parameters which controls the magnetic properties of this complex. In the configurational Interaction (CI) procedure, 21sextets, 140 quartets and 150 doublets are considered. In the RASSI module, 21 sextets, 128 quartets and 130 doublets are mixed by spin-orbit coupling. The active space for $[Tb^{III}(NO_3)_6]^{3-}$ [**2**] is 8 in 7 for the f^8 configuration of the Tb^{III} ion. In the CI procedure, the septets are given 7 roots, the quintets are given 140 roots and the triplets are given 195 roots. The singlet states were not included due to computational limitations. In the RASSI module all the states within the energy window of about 40,000 cm^{-1} (seven septets, 105 quintets and 112 triplets) were allowed to mix by spin-orbit coupling. Cholesky decomposition of the two-electron integrals was performed to save disk space. The active space for $[Ce^{III}(NO_3)_6]^{3-}$[**3**] is 1 in 7 for the f^1 configuration of Ce^{III} ion. The CI procedure includes 7 doublet and all of them are incorporated in the RASSI module. Our next complex of interest is $[Nd^{III}(NO_3)_6]^{3-}$[**4**] which has active space of 3 in 7 for

f^3 electronic configuration of Nd^{III} ion. In the CI procedure 35 quartets and 112 doublets are considered. In the RASSI module all the 35 quartets and 112 doublets are mixed by spin-orbit coupling. Our next complex of interest is $[Pr^{III}(NO_3)_6]^{3-}$[**5**] which has active space of 2 in 7 for f^2 electronic configuration of Pr^{III}. In the CI procedure, triplets are given 21 roots and singlets are given 28 roots. In the RASSI module all the 21 triplets and 28 singlets are mixed by spin-orbit coupling. Now, we will focus on complex $[Sm^{III}(NO_3)_6]^{3-}$ [**6**] which has active space of 5 in 7 for f^5 electronic configuration of Sm^{III} ion. The RASSI and CI calculation for Sm^{III} is similar to that for Dy^{III}. Structural optimization have been computed using DFT calculations employing Gaussian 09[45] suite. Here we have employed the B3LYP[46–48] functional, along with the Cundari-Stevens double ζ polarization basis set[49] for the Ln^{III} ions and the Ahlrichs triple ζ basis set[50] for the rest of the atoms.

3. Result and Discussion

Here we have chosen six structures **1**-**6** for our study. All the complexes comprise twelve coordinate Dy^{III},[51] Tb^{III},[52] Ce^{III},[53] Nd^{III},[54] Pr^{III}[55] and Sm^{III} in slightly distorted octahedron coordination environment surrounded by six symmetrically equivalent NO_3^- ligands (figure 1). The reported X-ray structure is taken as-is for calculations for all other structures except complex **6**. For complex **6**, the Ce^{III} analogue has been employed to model the Sm^{III} structure.

Among the lanthanide family, Dy^{III} ion has indisputably led to the largest number of pure SIMs.[10,56–58] The explanation resides in the reduced QTM observed in these systems compared to other lanthanide ions owing to its large magnetic moment and odd electron configuration. Here we start our discussion with individual lanthanide ions, and compare between lanthanide complexes later.

3.1 *Studies on complex 1*

The ground state Kramers Doublet (KD) is Ising in nature (g_{xx} = 0.04, g_{yy} = 0.06, g_{zz} = 15.34) for **1**. The first excited state KD possesses a large amount of transverse anisotropy and deviates largely with respect to the ground state anisotropy direction.

The energy spectrum and g-tensors for the first two Kramers doublets of the ground $^6H_{15/2}$ multiplet of the Dy^{III} ion in compound **1**, are shown in table 1, with excited multiplet $^6H_{13/2}$ lying at 3650 cm^{-1}. Effective energy barrier for relaxation of magnetization (U_{eff} or ΔE) in **1** is found to be 27.93 cm^{-1} (table 1) and this is
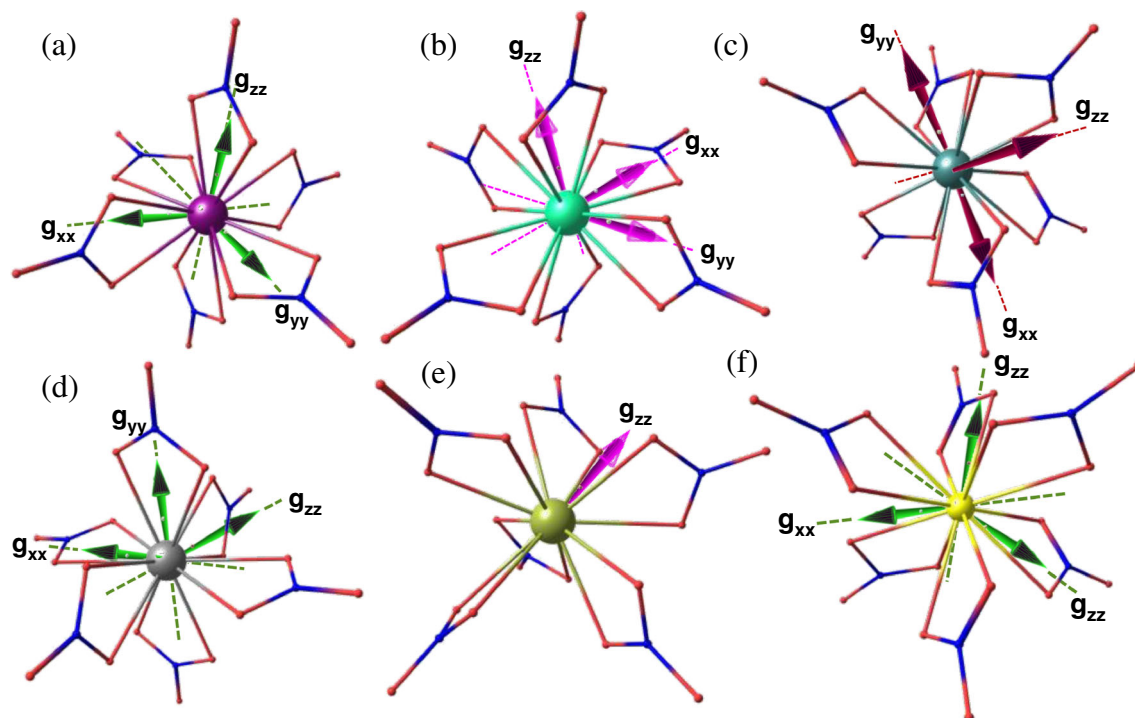
Figure 1. Showing direction of ground state anisotropy axis along X, Y and Z directions in [Ln^{III} (NO$_3$)$_6$]$^{3-}$ {where Ln^{III} = a) Dy(**1**), b) Tb(**2**), c) Ce(**3**), d) Nd(**4**) and f) Sm(**6**)}. Exceptionally, for complex **5** anisotropy only along the Z direction (g$_{zz}$) is shown for the fourth excited state, see text for details. (atomic colour scheme: Dy^{III}-purple, Tb^{III}-green, Ce^{III}-aqua, Nd^{III}-silver, Pr^{III}-yellowish green, Sm^{III}-yellow, O-red, N-blue).

in line with the experimental value reported for a similar structure.

3.2 *Variation of coordination number (C. N.) on Dy^{III}*

Pronounced dependence of magnetic anisotropy on the nature of counter-ions, ligands around the lanthanide ion, etc have been reported.[59–61] These results suggest that the magnetic behaviour of lanthanides depend on the structural changes around the ion.[59–61] Considering all these points, we have decided to extend our study

by varying the coordination number gradually from 12 to 2 around the lanthanide ion to observe the effect of ligation on the magnetic properties in complex **1-4**. All the structures possessing C. N. 11 to 2 are optimised using Gaussian 09[45] software suite (see section 2).

Analysing the changes of magnetic properties around Dy^{III} upon variation of C. N. (table 2 and figure 3b) we found that, among all the C. N. models tested, model with C. N. 11 shows the strongest transverse anisotropy. As we decrease the C. N. around Dy^{III}, a

Table 1. Calculated energy spectrum, g tensors, relative energies and angles(θ) of the principal anisotropy axes of first excited states with respect to the ground state for ground and fist excited Kramers (for **1,3,4,6**) and pseudo doublets (for **2** and **5**) in **1-6**.

Ground KDs /Non-KDs	1	2	3	4	5	6
g$_{xx}$	0.04	0	0.08	0.58	-	0.11
g$_{yy}$	0.06	0	0.53	1.73	-	0.47
g$_{zz}$	15.34	14.42	3.70	3.66	-	1.06
Relative energy (cm^{-1})	0.0	0.0 and 4.33	0.0	0.0	0.0	0.0
1st excited KDs /Non-KDs	1	2	3	4	5	6
g$_{xx}$	8.60	0	0.01	0.51	0	0.88
g$_{yy}$	8.56	0	0.94	0.70	0	0.59
g$_{zz}$	5.35	10.18	2.55	3.77	0	0.27
Relative energy (cm^{-1})	27.93	15.17 and 18.66	107.90	16.20	25.83	90.03
Angle {θ} (°)	0.10	98.60	40.41	85.30	-	52.78

Table 2. Calculated energy spectrum, g tensors and angles (θ) of the principal anisotropy axes of ground KDs of low valent Dy^{III} model complexes (from 11 to 2 C.N. change around Dy^{III} ion) with respect to their respective first excited state KDs.

Coordination no. around Dy in **1**	U_{eff} (cm^{-1})	g_x	g_y	g_z	Angle {θ} (°)
12	27.93	0.04	0.06	15.34	0.10
11	49.02	1.88	5.04	14.18	63.90
10	19.67	0.24	2.06	16.17	49.55
9	41.43	0.06	0.27	17.32	103.75
8	120.17	0.02	0.05	19.63	80.08
7	28.76	2.78	3.89	12.38	33.21
6	11.68	1.0	1.60	17.82	72.79
5	52.56	0.72	2.83	17.24	61.45
4*	420.04	0.0	0.0	19.81	163.40
3*	471.15	0	0	19.84	168.25
2*	410.48	0	0	19.86	2.87

*indicates barrier computed with second excited KDs due to collinearity with the first excited KDs.

gradual increase of Ising nature of anisotropy is attained till C. N. 8 model (figure 2). Further reduction of C. N. from 8 to 7 leads to an increase in rhombic anisotropy and for C. N. 6 and 5, a reduced rhombicity is observed (figure 3). As we go further down from C. N. 5 to lower Coordination Numbers, axial nature of the anisotropy is observed (for C. N. 2, 3 and 4 models). The angle between the direction of the excited state g_{zz} and the ground state g_{zz} is represented by tilt angle θ. Larger θ values suggest that the relaxation is predominantly happening via that particular KDs while smaller values reveal that the anisotropy is collinear and relaxation of magnetisation is likely to proceed via higher excited states leading to larger U_{eff} values.[62] This θ angle is found to be large for all the tested models except for models with C. N 2. Among all the C. N. models tested, model with C. N. 3 is found to possess highest U_{eff} values and this finding is in accordance with the recent synthesis of three coordinated Dy^{III} complexes possessing large U_{eff} value.[63] This observation highlights the importance of C. N. in fine tuning the U_{eff} values in lanthanide molecular magnets (figure 4a). Barring a few exceptions, we can conclude that C. N. variation is inversely proportional to the magnitude of U_{eff} values. We have also performed analysis on formation energies of all these varied coordinated complexes (figure 3a). We found that formation of model with C. N. 11 is most unfavourable, possessing highest positive formation energy (endothermic) with respect to C. N. 12 while the formation of C. N. 10 complex is most preferred (thermodynamically most stable compared to C. N. 12). This is in accordance with the experimental report where 10 co-ordination[53] Dy^{III} complexes are much more common than other coordination numbers. On the same note, except model with C. N. 8, formations of rest of the complexes are endothermic in nature. This is only a qualitative analysis on the stability of these models with respect to C. N. 12 as this analysis ignores the kinetics of formation and the likely variation in the ligand structures.

3.3 *Studies on complex 2*

Ground and first excited pseudo-doublet in **2** are of strong Ising nature with U_{eff} value computed to be 15.17 cm^{-1} (figure 4). Computed anisotropy for the first two pseudo doublet of the $^7F_6$ multiplet of the Tb^{III} ion in compound **2** is shown in table 1 with subsequent excited multiplet $^7F_5$ lying at 1990 cm^{-1}. The first excited pseudo-doublet forms a larger angle with respect to the ground state principal anisotropy directions. The tunnelling gap within the ground and first excited pseudo doublets are 4.33 and 3.49 cm^{-1} respectively.

3.4 *Variation of coordination number (C. N.) in Tb^{III}*

Being inspired by the effect of C.N. on the magnetic properties of the Dy^{III} models, we have performed a thorough analysis of gradual C.N. change around Tb^{III} in **2**. Independent of the C.N. all the ground state levels in **2** is found to be strongly Ising in nature, contrary to the behaviour observed for Dy^{III}. This unfolds an interesting observation that the Tb^{III} ground state anisotropy is unlikely to be influenced by the number of ligand atoms coordinated to the metal ions (table 3).

Among all the C. N. examined (figure 5), complex with C. N. 3 has been found to possess the largest U_{eff}
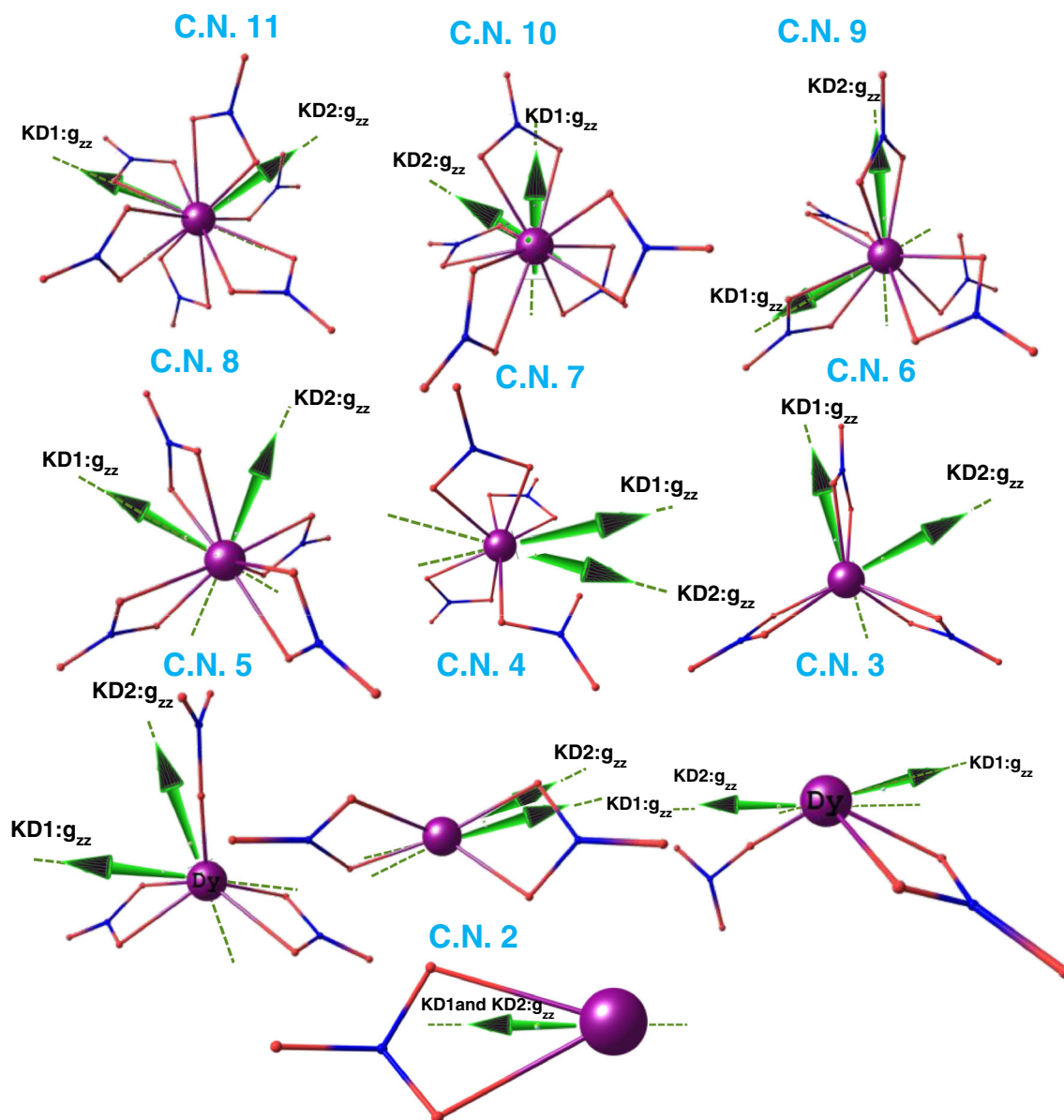
Figure 2. Model structures where C. N. varied from 11 to 2 around Dy^{III} in **1** along with the computed g$_{zz}$ direction for ground and first excited KD states.

values (270.52 cm^{-1}). This can be supported by recent trend and interest towards the synthesis of low valent lanthanide complexes.[63] The angle θ is found to be large for all the tested models. Here again, except a few cases, C. N. variation is inversely proportional to the magnitude of U$_{eff}$. Similar to complex **1**, we found that the formation of complex with C. N. 11 is most unfavourable possessing highest positive formation energy (endothermic) and formation of C. N. 10 complex is most preferred. On the same note, except complexes with C. N. 8 and 6, formations of rest of the complexes are endothermic in nature. From figure 4b, we can interpret that independent of C. N., in both **1** and **2** the magnitude of the g$_{zz}$ is inversely proportional to the

U$_{eff}$ value indicating intimate relationship between axial anisotropy and the relaxation energy barrier.

3.5 *Studies on Complex 3*

The energy spectrum and g-tensors for the Kramers doublets of the ground $^2F_{5/2}$ multiplet of Ce^{III} ion in **3** is shown in table 1 with excited multiplet $^2F_{7/2}$ lying at 2157 cm^{-1} higher in energy. Both the ground and first excited KD in **3** shows strongly rhombic nature of the anisotropy with large deviation of the first excited KD with respect to the ground state KD. Among the series of lanthanides studied by us, complex **3** is found to possess the highest U$_{eff}$ value (107.90 cm^{-1}).
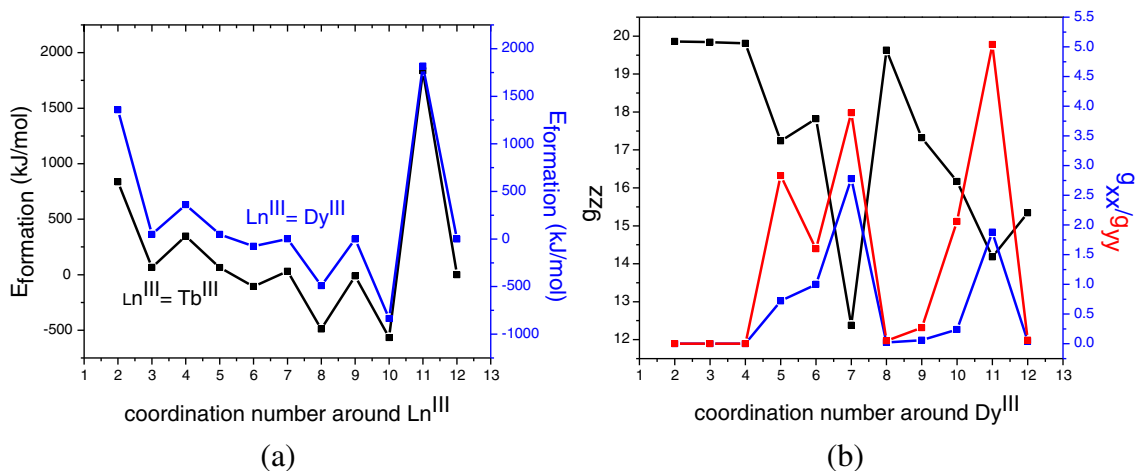
Figure 3. (a) Effect of gradual C.N. change from 12 to 2 on the formation energies for complexes **1** and **2**; (b) variation in the magnitude of g_{xx}, g_{yy} and g_{zz} values upon gradual change of C. N. from 12 to 2 around Dy^{III} ions in **1**.
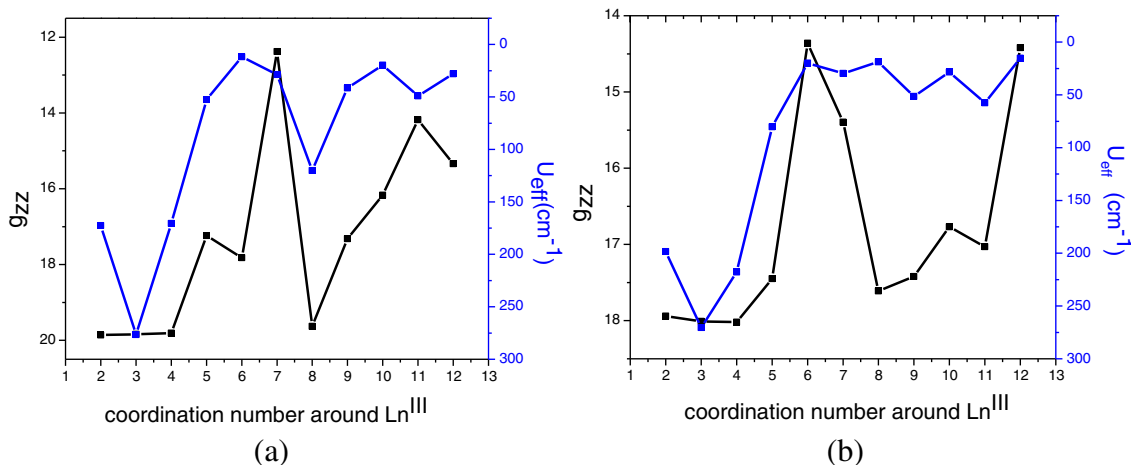

Figure 4. Dependence of C.N. on the magnitude of the effective energy barrier for relaxation along with ground state anisotropy direction along Z axis for (a) Dy^{III} and; (b) Tb^{III} ions.

3.6 *Variation of coordination number (C.N.) in Ce^{III}*

All the computed g-tensors and energy spectrum for varied coordinated complexes are shown in table 4.

Among all the C. N. studied (figure 5), complex with C.N. 2 model is found to possess the largest U_{eff} value. Model with C. N. 11 shows rhombic anisotropy while gradual increase in transverse nature of anisotropy is achieved till C. N. 9. Model with C.N. 7 possesses axial anisotropy followed by rhombicity in case of C.N. 6. As we further go down from C. N. 6 to 5, transverse anisotropic behaviour is observed again. Further reduction in C.N. around Ce^{III} in **3**, produces almost Ising behaviour. Independent of the C. N., the θ angle is found to be large for all tested models. Model with C.N. 5 is found to have largest transverse anisotropy whereas C. N. 2 has largest Ising anisotropy.

3.7 *Studies on complex 4*

The energy spectrum and g-tensors for the Kramers doublets of the ground $^4I_{9/2}$ multiplet of Nd^{III} ion computed for **4** is shown in table 1 with excited multiplet $^4I_{11/2}$ lying at 2157 cm^{-1} higher in energy. Ground state shows rhombic character whereas first excited state possesses axial anisotropy with U_{eff} value of 16.2 cm^{-1}. First excited anisotropy direction lies almost orthogonal with respect to the ground state Kramers Doublet.

3.8 *Variation of coordination number (C. N.) in Nd^{III}*

The energy spectrum and all computed values for versatile coordinated complexes are listed in table 5.

Model with C.N. 4 is found to possess the largest U_{eff} and also possesses axial ground state anisotropy and

Table 3. Calculated energy spectrum, g tensors and angles (θ) of the principal anisotropy axes of ground pseudo-doublets of Tb^{III} model complexes (from 11 to 2 C.N. change around Tb^{III} ion) with respect to their respective first excited state pseudo-doublets.

Coordination no. around Tb	U_{eff} (cm^{-1})	g_x	g_y	g_z	Angle {θ} (°)
12	15.17	0	0	14.42	98.59
11	57.63	0	0	17.03	18.68
10	28.37	0	0	16.77	35.97
9	96.49*	0	0	17.42	39.17
8	62.50*	0	0	17.61	60.46
7	29.64	0	0	15.396	35.30
6	19.89	0	0	14.36	9.55
5	80.297	0	0	17.45	89.76
4	336.92*	0	0	18.02	94.76
3	505.80*	0	0	18.01	11.85
2	308.48*	0	0	17.94	101.21

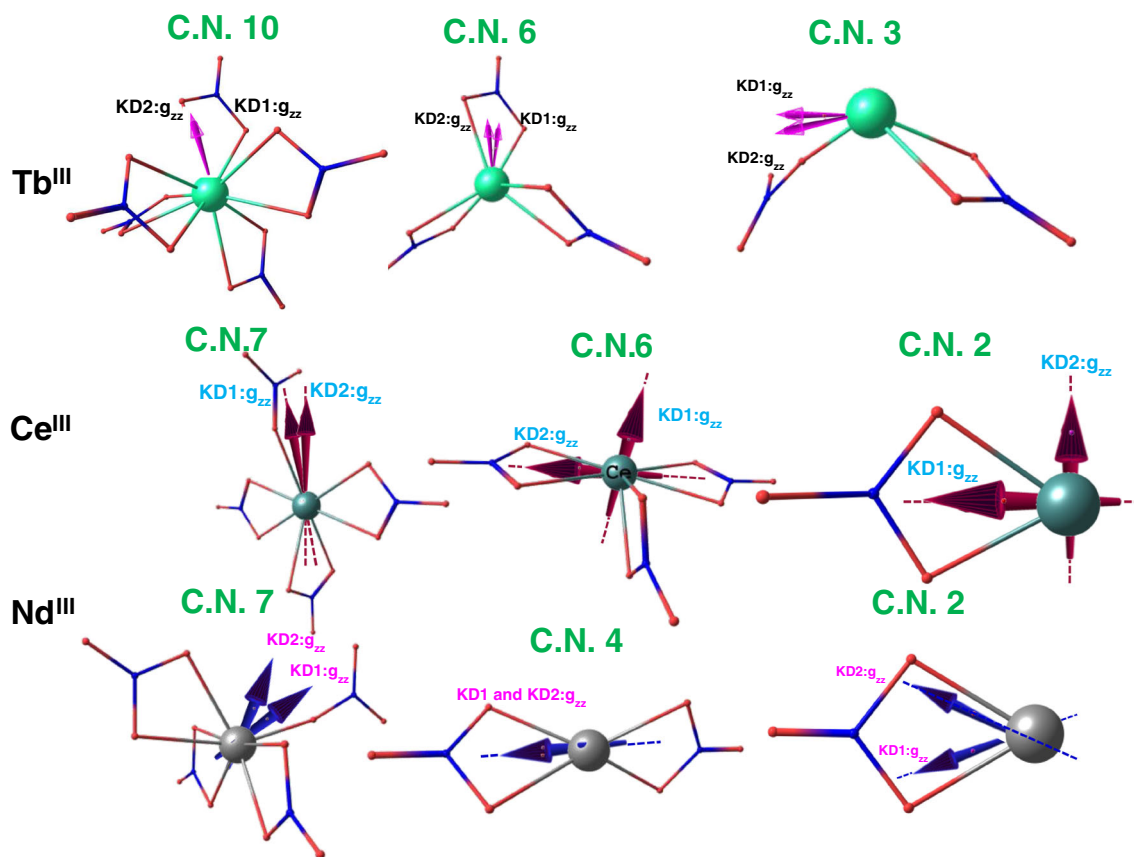*indicates barrier computed with second excited KDs due to collinearity with the first excited KDs.

Figure 5. Model structures where C. N is altered around Tb^{III}, Ce^{III}, and Nd^{III} in **2**, **3** and **4** along with the anisotropy directions of ground *vs.* first excited KDs/non-KDs.

have smallest θ angle (compared to other C. N. models). Models with C. N. 11 were found to possess rhombic anisotropy. As we decrease the C. N. around the Nd^{III}, a gradual increase in transverse nature of anisotropy is attained till C.N. 9. Further reduction of C. N. from 9 to 6 and 7 leads to an observation of rhombic nature of anisotropy. As we go further down from C.N. 5 to lower C. N number models, axial nature of the anisotropy is observed. The angle θ is found to be large for all tested models.

Table 4. Calculated energy spectrum, g tensors and angles (θ) of the principal anisotropy axes of ground KDs of Ce^{III} model complexes (from 11 to 2 C.N. change around Ce^{III} ion) with respect to their respective first excited state KDs.

Coordination no. around Ce	U_{eff} (cm^{-1})	g_x	g_y	g_z	Angle {θ} (°)
12	107.90	0.08	0.53	3.70	40.41
11	48.91	0.57	1.31	3.56	78.27
10	63.72	2.03	1.71	0.80	90.70
9[a]	89.41	2.06	1.02	0.20	26.14
7	431.76	0.54	0.59	3.72	14.78
6	381.92	0.63	1.14	3.90	90.53
5	299.14	2.46	2.24	0.83	20.19
4[a]	821.28	0.05	0.06	4.16	89.30
2	972.38	0.03	0.07	4.11	85.26

a) note here that C. N models 3 and 8 are missing as these models did not lead to minimum energy structures.

Table 5. Calculated energy spectrum, g tensors and angles (θ) of the principal anisotropy axes of ground KDs of Nd^{III} model complexes (from 11 to 2 C.N. change around Nd^{III} ion) with respect to their respective first excited state KDs.

Coordination no. around Nd	U_{eff}(cm^{-1})	g_x	g_y	g_z	Angle {θ} (°)
12	16.20	0.58	1.73	3.66	85.30
11	20.64	1.49	2.02	3.56	107.90
10	48.18	2.83	2.69	1.81	47.14
9[a]	37.24	2.30	2.49	1.44	47.94
7	87.24	0.22	1.02	3.91	23.87
6[a]	93.29	0.13	1.56	3.39	64.28
4[a]	416.64	0.03	0.07	4.73	66.37*
2	53.20	0.05	0.17	5.04	32.99

a) note here that C. N models 3, 5 and 8 are missing as these models did not lead to minimum energy structures.
*indicates barrier computed with second excited KDs due to collinearity with the first excited KDs.

3.9 *Studies on complex 5 and 6*

The energy spectrum and g-tensors for two pseudo-doublets and five singlets of the ground $^3H_4$ multiplet of Pr^{III} ion in **5** are shown in table 1 with excited multiplet $^3H_5$ lying at 2270 cm^{-1}. First three levels in **5** are singlet states and this precludes SMM behaviour for **5**. It is noteworthy that, only fourth and fifth levels are pseudo doublets with magnetic moment and these are Ising in nature. The energy spectrum and g-tensors for three KDs of the ground $^6H_{5/2}$ multiplet of Sm^{III} ion in **6** are shown in table 1 with excited multiplet $^6H_{7/2}$ lying at 1030 cm^{-1}. Effective energy barrier required for reorientation of magnetization is found to be 90.03 cm^{-1} in complex **6**. Ground state anisotropy is rhombic in nature with first excited state possessing significant transverse anisotropy. Ground state KD lies at a large θ

angle with respect to first excited KD in **6** resulting in possible relaxation via the first excited KDs.

4. Conclusions

We have performed fragment *ab initio* calculations on a series of lanthanide complexes [Ln^{III} = Dy(**1**), Tb(**2**), Ce(**3**), Nd(**4**), Pr(**5**) and Sm(**6**)] to shed light on the magnetic properties. Conclusions derived from our work are summarized below:

1) All the studied complexes except **5** are likely to exhibit SMM characteristics as significant barrier to reorientation of magnetisation is computed. However experimental observation of SMM behaviour may be hampered by QTM and intermolecular interactions.

2) The computed U_{eff} values for the five complexes are found to decrease in the order (**3**>**6**>**1**>**4**>**2**; U_{eff} 107.9>90.03>27.93>16.2>15.17 cm^{-1}) suggesting largest barrier height for Ce^{III} complex followed by Sm^{III}, Dy^{III}, Nd^{III} and Tb^{III}. The Dy^{III} and Sm^{III} are the best oblate and prolate ions respectively to exhibit SMM properties Thus it is not surprising that they possess large U_{eff} values. The Ce^{III} ion possesses oblate electron density and is predicted to yield only small U_{eff} values.[64] However here we predict that the Ce^{III} structure possesses the largest U_{eff} of the entire complex set tested. This is rather intriguing and unprecedented and requires an experimental verification.

3) Among the complexes studied, ground state anisotropy of complex **1** and **2** are Ising in nature while for **3**, **4** and **6**, a rhombic anisotropy is detected and complex **5** is not an SMM. The nature of anisotropy computed suggests that the tunnelling between the ground state KDs are likely to be small for complexes **1** and **2** while it is expected to be substantial for complexes **3**, **4** and **6**. This leads to larger QTM for **3**, **4** and **6** while relatively less for **1** and **2** and this effect may overshadow the computed U_{eff} values discussed above.

4) Analysing the trend among the models with variation in C. N. reveals an inverse correlation between C. N. and U_{eff} and g_{zz} values. In all the tested cases low-coordinate models yield substantially higher barrier heights and this suggests that these are likely to be superior SMMs over regular high coordination number structures. Thus synthetic efforts targeted towards low-coordinate lanthanide complexes should be pursued to obtain larger U_{eff} values.

5) Among all the complexes tested three coordinate Ce^{III} model is found to possess exceptionally large U_{eff} value of 972.38 cm^{-1} Although, it is challenging to synthesise low-coordinate Ce^{III} complexes, extremely large barrier height computed might make them a suitable synthetic target.

Supplementary Information

Supplementary information contains coordinates of all the DFT optimised model complexes studied for complex **1**, **3**, **4** and **6** and computational details. For further details, visit www.ias.ac.in/chemsci.

Acknowledgements

References

1. Leuenberger M N and Loss D 2001 *Nature* **410** 789
2. Saitoh E Miyajima H Yamaoka T and Tatara G 2004 *Nature* **432** 203
3. Yamanouchi M Chiba D Matsukura F and Ohno H 2004 *Nature* **428** 539
4. Evangelisti M Luis F de Jongh L J and Affronte M 2006 *J. Mater. Chem.* **16** 2534
5. Bogani L and Wernsdorfer W 2008 *NatMater* **7** 179
6. Manoli M Collins A Parsons S Candini A Evangelisti M and Brechin E K 2008 *J. Am. Chem. Soc.* **130** 11129
7. Ganivet C R Ballesteros B de la Torre G Clemente-Juan J M Coronado E and Torres T 2013 *Chem. Eur. J.* **19** 1457
8. Ishikawa N Sugita M and Wernsdorfer W 2005 *Angew. Chem. Int. Ed.* **44** 2931
9. Christou G Gatteschi D Hendrickson D N and Sessoli R 2000 *MRS Bull* **25** 66
10. Jiang S D Wang B W Su G Wang Z M and Gao S 2010 *Angew. Chem. Int. Ed.* **49** 7448
11. Jeletic M Lin P H Le Roy, J J Korobkov I Gorelsky S I and Murugesu M 2011 *J. Am. Chem. Soc.* **133** 19286
12. Jiang S D Wang B W Sun H L Wang Z M and Gao S 2011 *J. Am. Chem. Soc.* **133** 4730
13. Zhang P Guo Y N and Tang J K 2013 *Coord. Chem. Rev.* **257** 1728
14. Guo Z and Sadler P J 1999 *Angew. Chem. Int. Ed.* **38** 1512
15. Bornhop D J Hubbard D S Houlne M P Adair C Kiefer G E Pence B C and Morgan D L 1999 *Anal. Chem.* **71** 2607
16. Ishikawa N Sugita M Ishikawa T Koshihara S and Kaizu Y 2003 *J. Am. Chem. Soc.* **125** 8694
17. Ishikawa N Sugita M Ishikawa T Koshihara S and Kaizu Y 2004 *J. Phys. Chem. B* **108** 11265
18. Aromí G and Brechin E K 2006 *Struct. Bond* **122** 1
19. Gonidec M Luis F Vilchez A Esquena J Amabilino D B and Veciana J 2010 *Angew. Chem. Int. Ed.* **49** 1623
20. Rinehart J D and Long J R 2009 *J. Am. Chem. Soc.* **131** 12558
21. Guo Y N Xu G F Guo Y and Tang J K 2011 *Dalton Trans.* **40** 9953
22. Car P E Perfetti M Mannini M Favre A Caneschi A and Sessoli R 2011 *Chem. Commun.* **47** 3751
23. Rinehart J D Meihaus K R and Long J R 2010 *J. Am. Chem. Soc.* **132** 7572
24. Guo Y N Xu G F Wernsdorfer W Ungur L Guo Y Tang J K Zhang, H J Chibotaru L F and Powell A K 2011 *J. Am. Chem. Soc.* **133** 11948
25. Gatteschi D, Sessoli R J Villain 2006 In *Molecular Nanomagnets* (Oxford: Oxford University Press)
26. Sessoli R Gatteschi D Caneschi A and Novak M A 1993 *Nature* **365** 141

27. Sessoli R and Powell A K 2009 *Coord. Chem. Rev.* **253** 2328
28. Benelli C and Gatteschi D 2002 *Chem. Rev.* **102** 2369
29. Osa S Kido T Matsumoto N Re N Pochaba A and Mrozinski J 2004 *J. Am. Chem. Soc.* **126** 420
30. Zaleski C M Depperman E C Kampf J W Kirk M L and Pecoraro V L 2004 *Angew. Chem. Int. Ed.* **43** 3912
31. Tang J K Hewitt I Madhu N T Chastanet G Wernsdorfer W Anson C E Benelli C Sessoli R and Powell A K 2006 *Angew. Chem. Int. Ed.* **45** 1729
32. AlDamen M A Clemente-Juan J M Coronado E Marti-Gastaldo C and Gaita-Arino A 2008 *J. Am. Chem. Soc.* **130** 8874
33. Lin P H Burchell T J Clerac R and Murugesu M 2008 *Angew. Chem. Int. Ed.* **47** 8848
34. AlDamen M A Cardona-Serra S Clemente-Juan J M Coronado E Gaita-Arino A Marti-Gastaldo C Luis F and Montero O 2009 *Inorg. Chem.* **48** 3467
35. Gatteschi D and Sorace L 2001 *J. Solid State Chem.* **159** 253
36. Zvezdin A K Matveev V M, Mukhin A A and Popov A I 1985 In *Rare-earth ions in ordered magnetic crystals* (Moscow: Nauka) p 296
37. Gudel H U Hauser U and Furrer A 1979 *Inorg. Chem.* **18** 2730
38. Amoretti G Caciuffo R Carretta S Guidi T Magnani N and Santini P 2008 *Inorg. Chim. Acta* **361** 3771
39. Gatteschi D and Bencini A 1990 In *EPR of Exchange Coupled Systems* (Berlin: Springer-Verlag)
40. Barra A L Gatteschi D Sessoli R Abbati G L Cornia A Fabretti A C and Uytterhoeven M G 199 *Angew. Chem. Int. Ed.* **36** 2329
41. Aquilante F De Vico L Ferre N Ghigo G Malmqvist P A Neogra024dy P Pedersen T B Pitonak M Reiher M Roos B O Serrano-Andres L Urban M Veryazov V and Lindh R 2010 *J. Comput. Chem.* **31** 224
42. Bernot K Luzon J Bogani L Etienne M Sangregorio C Shanmugam M Caneschi A Sessoli R and Gatteschi D 2009 *J. Am. Chem. Soc.* **131** 5573
43. Cucinotta G Perfetti M Luzon J Etienne M Car P E Caneschi A Calvez G Bernot K and Sessoli R 2012 *Angew. Chem. Int. Ed.* **51** 1606
44. Boulon M-E Cucinotta G Luzon J Degl'Innocenti C Perfetti M Bernot K Calvez G Caneschi A and Sessoli R 2013 *Angew. Chem. Int. Ed.* **125** 368
45. Gaussian 09, Revision **D.01**, Frisch M J, Trucks G W, Schlegel H B, Scuseria G E, Robb M A, Cheeseman J R, Scalmani G, Barone V, Mennucci B, Petersson G A, Nakatsuji H, Caricato M, Li X, Ratchian H P, Izmaylov A F, Bloino J, Zheng G, Sonnenberg J L, Hada M, Ehara M, Toyota K, Fukuda R, Hasegawa J, Ishida M, Nakajima T, Honda Y, Kitao O, Nakai H, Vreven T, Montgomery J A Jr., Peralta J E, Ogliaro F, Bearpark M, Heyd J J, Brothers E, Kudin K N, Staroverov V N, Kobayashi R, Normand J, Raghavachari K, Rendell A, Burant J C, Iyengar S S, Tomasi J, Cossi M, Rega N, Millam N J, Klene M, Knox J E, Cross J B, Bakken V, Adamo C, Jaramillo J, Gomperts R, Stratmann R E, Yazyev O, Austin A J, Cammi R, Pomelli C, Ochterski J W, Martin R L, Morokuma K, Zakrzewski V G, Voth G A, Salvador P, Dannenberg J J, Dapprich S, Daniels A D, Farkas Ö, Foresman J B, Ortiz J V, Cioslowski J, Fox D J Gaussian, Inc., Wallingford CT, 2009
46. Lee C T Yang W T and Parr R G 1988 *Phys. Rev. B* **37** 785
47. Becke A D 1993 *J. Chem. Phys.* **98** 5648
48. Stephens P J Devlin F J Chabalowski C F and Frisch M J 1994 *J Phys Chem Us* **9** 11623
49. Cundari T R and Stevens W J 1993 *J. Chem. Phys.* **98** 5555
50. Schafer A Huber C and Ahlrichs R 1994 *J. Chem. Phys.* **100** 5829
51. Chekhlov A N 2007 *Russ. J. Inorg. Chem.* **52** 1741
52. del C Fernández-Fernández M Bastida R Macías A Pérez-Lourido P Platas-Iglesias C and Valencia L 2006 *Inorg. Chem.* **45** 4484
53. Cui H Otsuka T Kobayashi A Takeda N Ishikawa M Misaki Y and Kobayashi H 2003 *Inorg. Chem.* **42** 6114
54. Lu W-J Zhang L-P Chan H-S Chan T-L and Mak T C W 2004 *Polyhedron* **23** 1089
55. Hamada T Manabe K Ishikawa S Nagayama S Shiro M and Kobayashi S 2003 *J. Am. Chem. Soc.* **125** 2989
56. Wang Y-L Gu B, Ma Y Xing CWang Q-L Li L-C Cheng P and Liao D-Z 2014 *CrystEngComm* **16** 2283
57. Ren M Pinkowicz D Yoon M Kim K Zheng L M Breedlove B K and Yamashita M 2013 *Inorg. Chem.* **52** 8342
58. Chen G J Guo Y N Tian J LTang J Gu W Liu X Yan S P Cheng P and Liao D Z 2012 *Chem. Eur. J.* **18** 2484
59. Binnemans K Malykhina L Mironov V S Haase W Driesen K Van Deun R Fluyt L Görller-Walrand C and Galyametdinov Y G 2001 *Chem. Phys. Chem.* **2** 680
60. Bünzli J-C G and Piguet C 2002 *Chem. Rev.* **102** 1897
61. Murugesu M 2012 *NatChem* **4** 347
62. Blagg R J Ungur L Tuna F Speak J Comar P Collison D Wernsdorfer W McInnes E J L Chibotaru L F and Winpenny R E P 2013 *Nat. Chem.* **5** 673
63. Zhang P Zhang L Wang C Xue S Lin S-Y and Tang J 2014 *J. Am. Chem. Soc.* **136** 4484
64. Rinehart J D and Long J R 2011 *Chem.Sci.* **2** 2078
65. (a) Herrmann W A, Anwander R, Munck F C, Scherer W, Dufaud V, Huber N W and Artus G R 1994 *J Z Naturforsch. B* **49** 1789; (b) Bradley D C, Ghotra J S and Hart F A 1972 *J. Chem. Soc. Chem. Commun.* 349
66. Zhang P, Zhang L, Wang C, Xue S, Lin S-Y and Tang J 2014 *J. Am. Chem. Soc.* **136** 4484
67. Sundararajan M, Ganyushin D, Ye S and Neese F 2009 *Dalton Trans* 6021
68. (a) Duncan J A 2009 *J. Am. Chem. Soc.* **131** 2416; (b) Aquilante F, De Vico L, Ferre N, Ghigo G, Malmqvist P A, Neogra024dy P, Pedersen T B, Pitonak M, Reiher M, Roos B O, Serrano-Andres L, Urban M, Veryazov V and Lindh R 2010 *J. Comput. Chem.* **31** 224; (c) Veryazov V,Widmark P O, Serrano-Andres L, Lindh R and Roos B O 2004 *Int. J. Quantum Chem.* **100** 626; (d) Karlstrom G, Lindh R, Malmqvist, P A, Roos B O, Ryde U, Veryazov V, Widmark P O, Cossi M, Schimmelpfennig B, Neogra024dy P and Seijo L 2003 *Comp. Mater. Sci.* **28** 222
69. Malmqvist P A, Roos B O and Schimmelpfennig B 2002 *Chem. Phys. Lett.* **357** 230
70. Chibotaru L F and Ungur L 2012 *J. Chem. Phys.* **137** 064112